Thermodynamic studies of anion adsorption at the Pt(111) electrode surface from glycolic acid solutions

Rosa M. Arán-Ais, Enrique Herrero, Juan M. Feliu

Instituto de Electroquímica, Universidad de Alicante, Apdo. 99, E-03080 Alicante, Spain

Abstract

Kinetic glycolic acid (GA) oxidation and thermodynamic glycolate adsorption have been studied on Pt single crystal electrodes. The voltammetric profiles of Pt(111), Pt(100) and Pt(110) in 0.1 M GA are shown, and the effect of the inclusion of steps on the Pt(111) surface has been studied by cyclic voltammetry. For Pt(111) electrode, different concentrations and sweep rates have been applied, revealing that both adsorption and oxidation processes take place. By establishing the appropriate conditions, a complete thermodynamic analysis has been performed by using the electrode potential and the charge as independent variables. Total charge density curves, surface pressure at total charge density and at constant electrode potential were determined to calculate the Gibbs excess and the charge number at constant electrode potential for glycolate adsorption on Pt(111). Maximum glycolate coverage on the surface reaches a value of ~ 6.0 $\times 10^{14}$ ions/cm^2. Spectroscopic results show the formation of CO_2 during the oxidation of glycolic acid, indicating that the cleavage of the C-C bond occurs during the oxidation process.

Keywords

Glycolic acid; Pt single crystals electrodes; Stepped surfaces; Thermodynamic study; In situ FTIR.

Introduction

Over the past decades, single crystal electrodes have been widely characterized using cyclic voltammetry (CV) as main technique. In the case of platinum electrodes, the voltammetric profile in the supporting electrolyte is extremely sensitive to the surface structure, allowing a qualitative assessment of the quality of the single crystal. For this metal, the improvement in the methodology for obtaining single crystal electrodes has continuously increased since the discovery of the flame annealing treatment [1,2]. The combination of the use of less defective single crystals electrodes and the use of solutions of higher purity has had their effect in the voltammetry with a significant diminution of the observed defects, leading to sharper and more symmetric features.

The electrochemical characterization of the electrodes is important because it can be used to determine the species adsorbed on the interface, which in turn affect the electrocatalytic response of the electrode. Thus, the voltammetric profile of the Pt(111) electrode and the nature of the species involved in the charge transfer processes have been studied in the different supporting electrolytes [2-4]. The sharp spike observed in its voltammetric profile in sulfuric acid containing solutions constitutes the best known example of the influence of the long-range order of the electrode surface on anion adsorption phenomena [5]. Anion coadsorption plays a key role in the building of the adlayer and affects dramatically the reactivity of the surface for the so-called structure sensitive processes. Ethanol and ethylene glycol oxidation reactions belong to this type of processes, and the competitive anion adsorption influences the reaction rate and also the mechanism. Since this coadsorption process is surface sensitive, the effects of this process on the different electrodes for the studied reaction are, therefore, also dependent on the surface structure [6]. Over the past year, there has been an increasing interest of these reactions on acidic media because of their potential application on direct alcohol fuel cells using an acidic polymer electrolyte membrane. Among the platinum single crystal electrodes used, Pt(111) seems to be the most reluctant to produce CO_2 in the direct oxidation of ethanol and ethylene glycol, being acetic acid and glycolic acid (GA) almost the only final products, respectively [6,7]. These latter products show voltammetric profiles characteristic of anion

adsorption/desorption processes, since their oxidation on platinum only takes place at significant rates at very high potentials. However, the inclusion of an OH group on the glycolic acid molecule (in comparison with acetic acid) makes it more reactive through the C-C bond cleavage, being possible to observe small oxidation currents when solutions of low concentration are used and/or when slow scan rates are applied [8].

This paper is a part of a broader project on thermodynamic studies of the adsorption of anions and their co-adsorption with cations at Pt(hkl) electrodes. Previous work from this series described sulfate/bisulfate adsorption at Pt(111) [9] and Pt(hkl) [10], adsorption of hydrogen and OH [3,11] and chloride adsorption at the Pt(111) surface [12]. Here we report on glycolate adsorption at the Pt(111) electrode. Integration of the cyclic voltammograms has been used to determine the amount of adsorbates at the electrode surface and the curves q vs. E. A full thermodynamic analysis has been performed, using the charge and the electrode potential as the electrical independent variables. The thermodynamic method has been used to determine the Gibbs excess of adsorbed species. When this method is used to measure the amount of adsorbed anion, the requirement that must be fulfilled is that, at least at one potential value (usually close to the onset of hydrogen evolution), the anion is totally desorbed from the electrode surface in all solutions investigated. Finally, the Gibbs excess data were employed to calculate the charge numbers at a constant potential (electrosorption valency).

There are several new elements that this work brings about to the knowledge of glycolic acid oxidation and glycolate adsorption on Pt single crystal electrodes. In the present paper, we will use the thermodynamic approach to gain quantitative insight into glycolate adsorption on the Pt(111) electrode. To do this, kinetic contributions should be avoided by applying certain conditions of work. Kinetic effects of glycolic acid oxidation will be examined by cyclic voltammetry at different sweep rates, and will be combined with FTIR experiments to identify the intermediates and products of this reaction.

Experimental

Pt(hkl) surface were used as working electrodes to carry out all the electrochemical experiments. Reported results are mainly given from Pt(111) and stepped surfaces vicinal to the (111) pole. As usual, the electrodes were made by fusion and subsequent slow crystallization of a 99,999% platinum wire which, after careful cooling, were cut and polished following the procedure described in reference [13]. Prior to each experiment, the working electrode was flame-annealed in a gas-oxygen flame, cooled down in a reductive atmosphere (H_2+Ar at a 1:3 ratio) and quenched in ultrapure water in equilibrium with this atmosphere before transferring to the electrochemical cell. Experiments were performed at room temperature in a classical two-compartment electrochemical cell, de-aerated using argon (Air Liquid, N50). The counter electrode was a platinum wire and the potentials were measured against a reversible hydrogen (Air Liquid, N50) electrode (RHE) connected to the cell through a Luggin capillary. Solutions were prepared from perchloric acid (Merck Suprapur®) and glycolic acid (GA, Sigma Aldrich, 99%) in ultrapure water from Elga. In the thermodynamic experiments, perchloric acid 0.1M was used as supporting electrolyte, to which 10 different GA concentrations were added in the range from 10^{-4} to 10^{-1} M to determine the Gibbs excess of adsorbed glycolate. At least three experiments were performed for each concentration. The electrode potential was controlled using an EG&G PARC 175 signal generator in combination with an eDAQ EA 161 potentiostat and currents were recorded using an eDAQ e-corder ED401 recording system.

Spectroelectrochemical experiments were performed with a Nicolet Magna 850 spectrometer equipped with a MCT detector. The spectroelectrochemical cell was provided with a prismatic CaF_2 window beveled at 60º. Spectra shown are composed of 200 interferograms collected with a resolution of 8 cm^{-1} and p polarized light. They are presented as absorbance, according to $A = -\log(R/R_0)$ where R and R_0 are the reflectance corresponding to the single beam spectra obtained at the sample and reference potentials, respectively. All the spectroelectrochemical experiments were also performed at room temperature, with a reversible hydrogen electrode (RHE) and a platinum wire used as reference and counter electrodes, respectively.

Results and discussion

Voltammetric behavior of the basal planes and stepped surface electrodes.

Fig. 1 shows the cyclic voltammograms (CVs) of the well ordered Pt(111), Pt(100) and Pt(110) surfaces in a 0.1 M GA + 0.1 M $HClO_4$ solution. As can be seen, the profiles obtained are almost identical to those measured in acetic acid solutions with the same pH [14]. Due to the similarity of their molecular structures, adsorption behavior is very similar, leading to almost identical CVs. In spite of the low pH solution and the low dissociation constant of the glycolic acid (pK_a=3.83), the results obtained clearly indicate the presence of specifically adsorbed anions. In the present experimental conditions, glycolate is the only anion that can be adsorbed on the electrode surface.

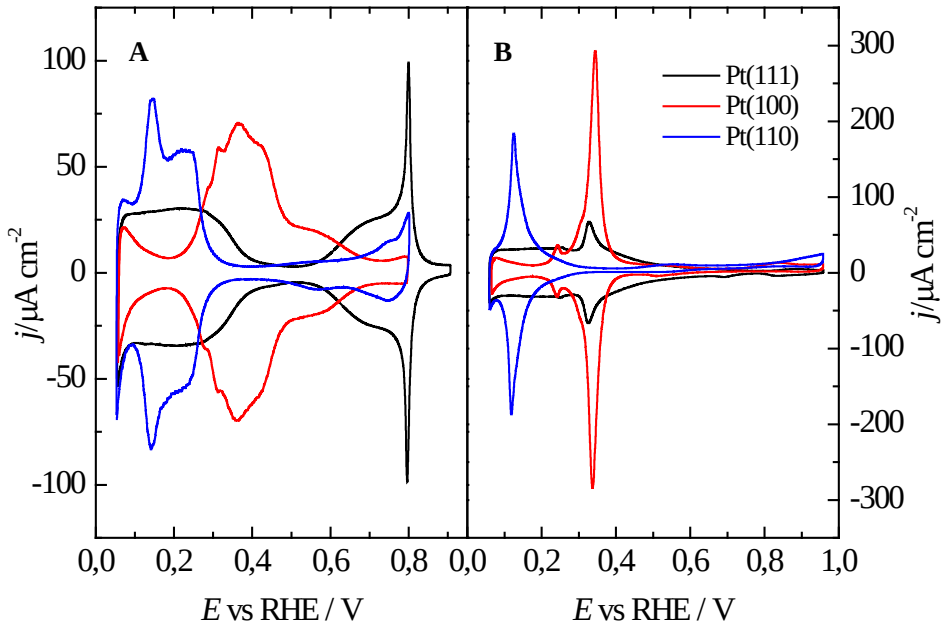

Fig. 1 Cyclic voltammograms for Pt(111), Pt(100) and Pt(110) electrodes in (A) 0.1 M $HClO_4$ and (B) 0.1 M GA + 0.1 M $HClO_4$. Sweep rate = 50 mV s^{-1}. Potentials measured vs RHE.

When compared to the voltammetric profiles measured in pure perchloric acid solutions, the addition of GA leads to the sharpening and shifting towards lower potential values of the

adsorption states in the hydrogen region for the Pt(100) and Pt(110) surfaces. This fact points out clearly to the adsorption of GA, which takes place at potentials more positive than the main peaks in the voltammogram, namely above 0.35 V and 0.12 V for the Pt(100) and Pt(110) electrodes, respectively. The presence of sharp peaks in those CVs are associated to the competitive adsorption of hydrogen and anion. At potentials close to the onset of hydrogen evolution, hydrogen is adsorbed on the surface and these species are replaced by adsorbed anions as the potential is scanned in the positive direction giving rise to the appearance of sharp peaks [15]. The absence of significant currents at potentials above 0.5 V indicates that the oxidation of GA for these electrodes and solutions is almost negligible.

The behavior of the Pt(111) electrode is slightly different, since the overlap of the potential windows in which hydrogen and anions adsorption is very small and both processes can be easily separated. The so-called unusual states can be considered as the beginning of the glycolate adsorption and it merits to be studied in more detail. For that reason, the behavior of Pt(111) electrode and its vicinal surfaces is shown in figure 2. In this figure, the effect of the presence of steps with (100) and (110) symmetry on the voltammetric response is clearly observed. In both cases, as the step density increases, the feature associated with glycolate adsorption on (111) sites decreases and moves towards more positive potentials, while the signal related with hydrogen adsorption on the step sites increases. It should be highlighted that the adsorption states on {100} steps are sharper and more intense than on {110} sites. For the {100} defect sites, the sharp peak points out to the presence of a competitive adsorption process between hydrogen ad glycolate on these steps. This would point out a stronger sensitivity to the adsorption of glycolate on {100} sites as compared to {110} ones and also to a stronger competition between hydrogen and anion adsorption.

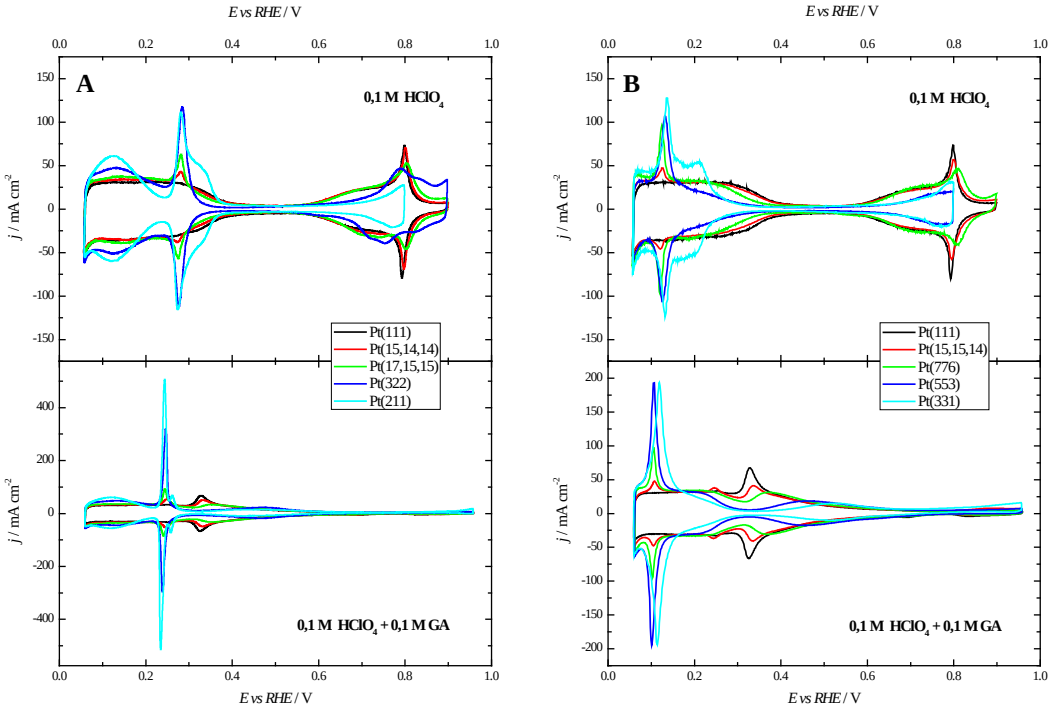

Fig. 2 Cyclic voltammograms for Pt(111) and its vicinal surfaces with monoatomic steps of (A) (100) and (B) (110) symmetry in 0.1 M $HClO_4$ (top) and in 0.1 M GA + 0.1 M $HClO_4$ (bottom) solutions. Sweep rate = 50 mV s^{-1}.

Before carrying out the thermodynamic analysis of the adsorption of glycolate, the conditions to obtain reliable data have to be assured. It has been pointed out that the presence of a OH group in the molecule of glycolic acid makes it more reactive on the Pt(111) surface in comparison with acetic acid, where only adsorption processes take place at potentials below 1 V [8]. Thermodynamic studies require equilibrium adsorption conditions and this is usually associated to voltammograms recorded at low sweep rates or charge measurements at constant potential. However, in the case of glycolic acid, oxidation currents are small albeit measurable when slow sweep rates are applied and/or diluted solutions are used. Thus, under those conditions it is possible to distinguish between thermodynamically controlled processes (hydrogen and anion adsorption) and kinetically controlled processes (glycolic acid oxidation). Fig. 3 shows the influence of the sweep rate on the voltammetric profiles for diluted and more concentrated solutions of GA. The current density values are normalized to the sweep rate for comparison. It can be seen that “pure” adsorption/desorption processes can be observed only

when concentrated solutions of GA are used (Fig. 3A), and that they are independent of the sweep rate applied, as it is expected for a thermodynamically controlled process. However, when low concentrations of GA are employed (Figs. 3B and 3C), both processes, thermodynamic adsorption and kinetic oxidation, can be observed. Thus, while the hydrogen adsorption (below 0.37 V) and the anion adsorption (broad state around 0.45 V) are not affected by the sweep rate normalization, the kinetic processes, which take place above 0.6 V, are more noticeable as potential is scanned at lower rates. The experiments in figure 3 show that the charge contribution of the oxidation process is almost negligible 50 mV/s, providing the lower limit for the scan rates that can be used for thermodynamic studies.

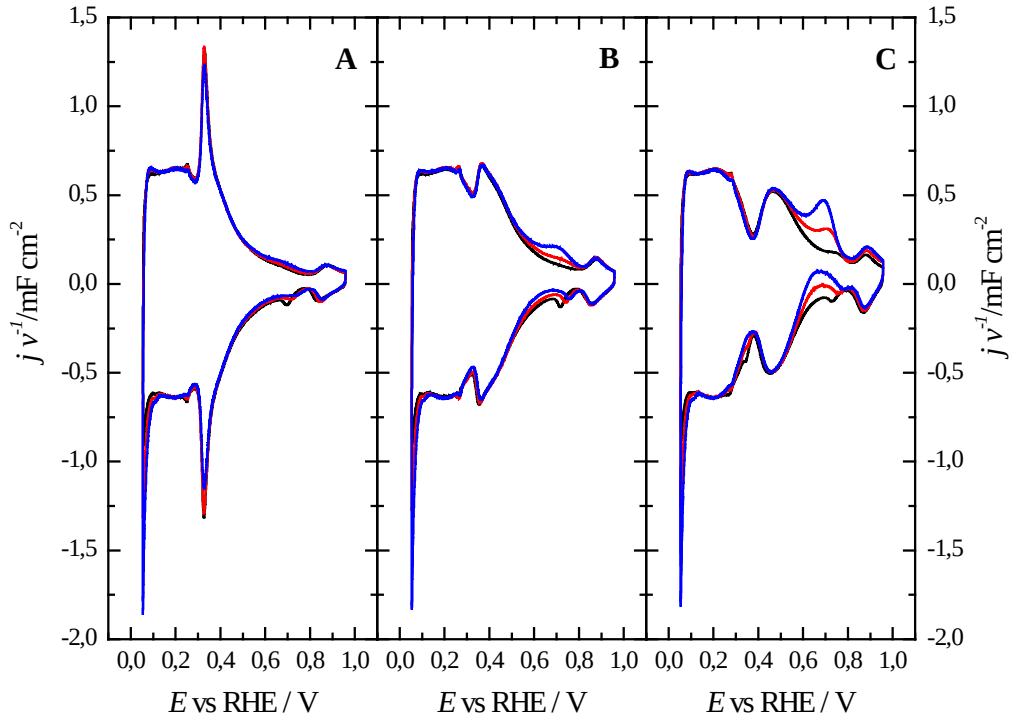

Fig. 3 Cyclic voltammograms recorded at the Pt(111) electrode at different sweep rates: 50 mV s^{-1} (black), 20 mV s^{-1} (red) and 10 mV s^{-1} (blue). Density currents are normalized by sweep rate to maintain constant the adsorption process and differentiate the kinetic contributions. Test solution: 0.1 M $HClO_4$ with (A) 0.1 M GA, (B) 10^{-2} M GA and (C) 10^{-3} M GA.

Thermodynamic analysis of the adsorption of glycolate

Once the conditions to obtain reliable voltammograms for thermodynamic studies have been established, the surface concentrations of the adsorbed anion can be calculated from voltammetry. Fig. 4 shows representative voltammetric profiles for Pt(111) electrode in solutions of pure 0.1 M perchloric acid and with different GA concentrations. The concentration of GA was progressively increased from 1.0×10^{-4} M to 1.0×10^{-1} M. The Pt(111) electrode used was a high quality one, as revealed by the shape of the CV in pure perchloric acid, characteristic of a defect-free surface [3]. Absence of defects is required to have a reference potential region in which the surface could be considered free of adsorbed anions. As aforementioned, a relatively high sweep rate (50 mV s^{-1}) was required to discriminate thermodynamic processes, thus mainly adsorption/desorption states are taken into account in the range of potentials studied. Within the hydrogen adsorption region (at E < 0.3 V), the curves recorded in different solutions overlap nicely. Indeed, this feature indicates an excellent reproducibility, probes that the oxygen content in the electrolyte is low and shows that glycolate anions are totally desorbed from the electrode surface in this potential region. The currents associated to the anion adsorption grows and shifts towards the negative values when the bulk concentration of GA increases, becoming a sharp and well-defined peak that mimics the well-known 'butterfly' feature, characteristic for (bi)sulfate [9], acetate [14,16], tetrafluoroborate [17] and chloride [12] adsorption at the Pt(111) electrode surface, just to indicate fewer examples. For solutions with GA concentrations higher than 5×10^{-4} M, the CVs recorded display good symmetry indicating good reversibility of the adsorption/desorption phenomena. The performed measurements at lower sweep rates (Fig.3) pointed out that the irreversibility observed for solutions with low GA concentrations is due to the kinetic oxidation process and not to a slow mass transport to the surface. However, it can be considered that data in the potential region higher than 0.6 V obtained for GA concentrations lower than 10^{-3} M contain some small contributions from GA oxidation. It should be noted that the traditional charge integration from j-t potentiostatic curves could not be applicable at these conditions in this potential range.

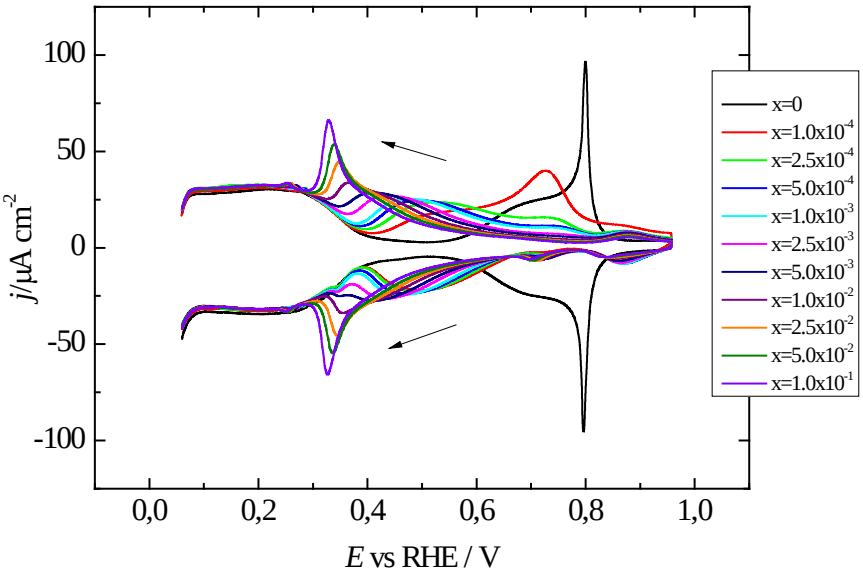

Fig. 4 Cyclic voltammograms recorded at the Pt(111) electrode in solutions *x* M GA + 0.1 M $HClO_4$. Sweep rate, 50 mV s^{-1}. Arrows indicate the directions in which the current increases with the bulk GA concentration.

The CVs represented on Fig. 4 were integrated in order to obtain the total charge density at the electrode surface *q*. The potential of the total zero charge for the Pt(111) on a pure 0.1 M $HClO_4$ solution, determined by the CO displacement method, is equal to 0.34 V [18] and can be used as the integration constant. In addition, it was assumed that at E = 0.1 V, where glycolate anions are totally desorbed from the electrode surface (as conclude from the CV), charge densities are independent of the presence of GA in the mixed electrolyte and consequently are the same as those measured in perchloric acid. When CVs are used to determine the electrode charge density, it is necessary to take into account two possible sources of error. The first one is related with the residual faradaic current mainly caused by the presence of traces of oxygen in the solution. To eliminate this problem, charge curves were obtained from the integration of the average of the positive and negative going sweeps of the CVs. The second one is related to the reversibility of the glycolate adsorption/desorption at concentrations lower than 5×10^{-4} M. It was checked that values of the surface excesses calculated with and without those

concentrations in the relevant region were the same within the error of the calculations. In order to show global trends, those concentrations were maintained in the figures.

. The total charge density curves are represented in Fig. 5. They constitute the fundamental set of data for the subsequent thermodynamic analysis. At potentials lower than 0.3 V, the curves determined for different solutions merge into a line as hydrogen is thermodynamically adsorbed and pH is constant in all solutions. This important feature indicates an excellent reproducibility of the experimental conditions throughout the whole series of measurements. At potentials above 0.3 V, the charge density curves display a characteristic step indicating anion adsorption at the Pt surface. The charge increases gradually with potential for all GA solutions, merging into a quasi-plateau at E ~ 0.79V, where all the curves (except the one belonging to the lowest concentration) intersect the curve of the supporting electrolyte. The behavior of the lowest concentration determines the limits for the reliability of the present experimental data coming from high sweep rate voltammograms.

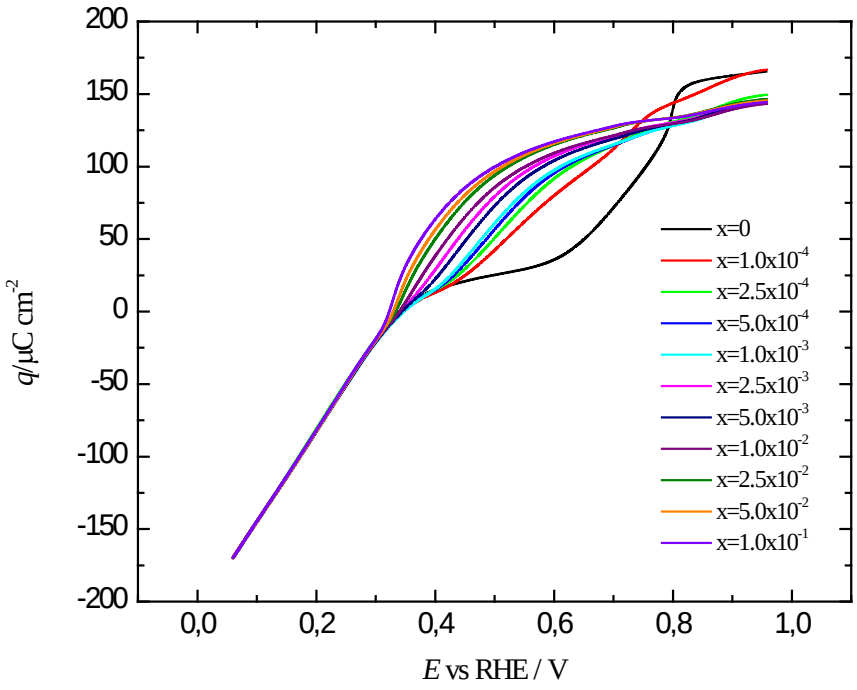

Fig. 5 Total charge density of Pt(111) plotted against the electrode potential from integration of the voltammograms of Fig. 2. GA concentration increases from right to left.

When experiments are carried out in solutions of a constant pH and a constant ionic strength, the electrocapillary equation for the Pt | GA-containing solution interface is described by [19]:

$$\Gamma = \left(\frac{\partial \gamma}{\partial RT \ln c_{GA}}\right)_{q} \quad (1)$$

where γ is the surface energy, q is the total charge density at the electrode surface and Γ_{GA} is the Gibbs excess of specifically adsorbed glycolate. Eq. (1) shows that the Gibbs excess Γ_{GA} can be determined by differentiation of γ with respect to RT ln c_{GA}. It is possible to calculate the surface pressure of adsorbed anions $\pi = \gamma_{\theta=0} - \gamma_{\theta}$ by integration of the curves of Δq vs.E [19]:

$$\pi_{\theta=0} - \pi_{\theta} = \int_{\theta=0}^{\theta} -q \, dE \quad (2)$$

where subscripts θ = 0 and θ denote the values of the surface energy and the total charge density measured in pure 0.1 M $HClO_4$ and 0.1 M $HClO_4$ + x M GA solutions, respectively.

When the charge is considered as the independent electrical variable [20] is possible to use the Parsons function $\xi = \sigma_{ME} + \gamma$ to calculate the Gibbs excess. In that case, the surface pressure at constant charge is obtained with the help of the following equation:

$$\xi_{\theta=0} - \xi_{\theta} = \gamma_{\theta=0} - \gamma_{\theta} = \int_{\theta=0}^{\theta} -q \, dE \quad (3)$$

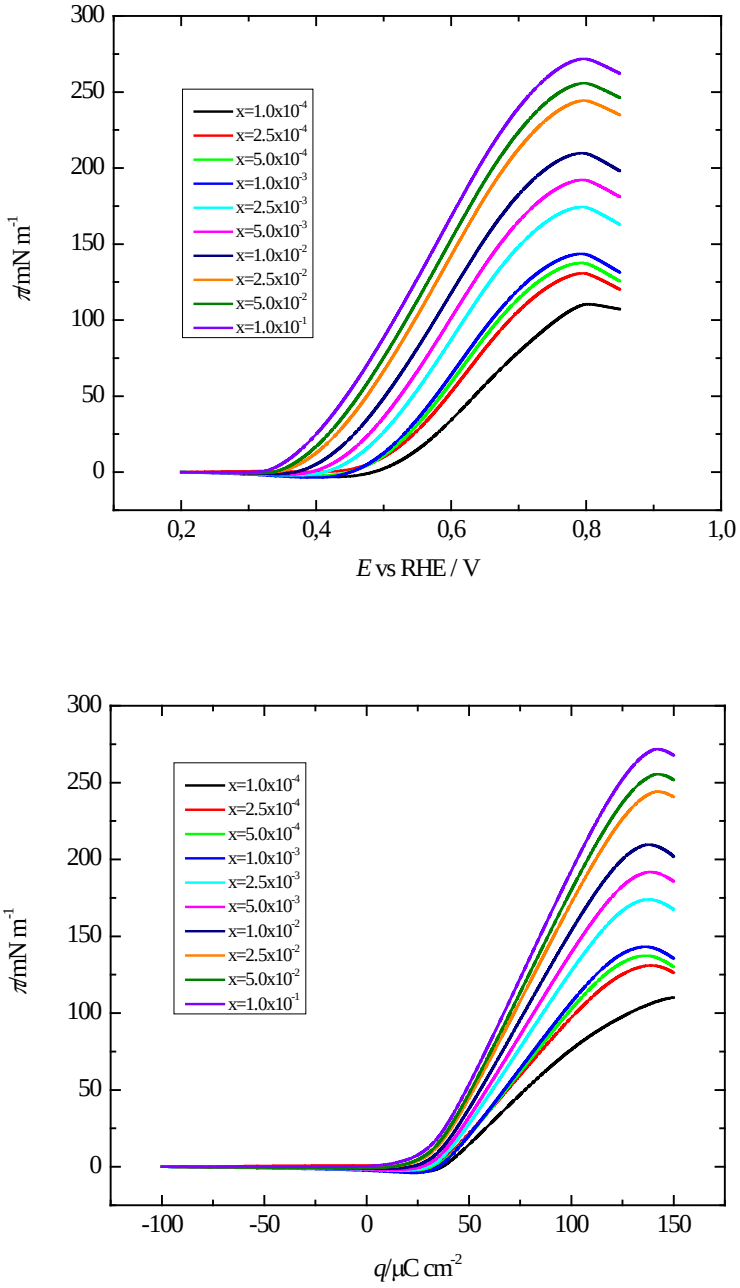

Fig. 6 Surface pressure, π, plotted against (A) total charge density and (B) electrode potential, for GA adsorption at Pt(111) surface from charges in Fig. 3. GA concentration decreases from top to the bottom.

The surface pressures calculated by using Eq. (2) and Eq. (3) are represented in Fig. 6A and 6B, respectively. It should be noted that surface pressures at either constant potential or charge increases as the bulk concentration of GA is increased, displaying a maximum when

plotted against the corresponding electrical variable. These coordinates are the charge and the potential of maximum adsorption, respectively.

The Gibbs excess of adsorbed glycolate can now be determined by plotting the surface pressure at constant total charge as a function of RT ln c_{GA} and differentiating these plots. Fig. 7 plots π vs. $RT\ ln\ c_{GA}$, for selected charge densities. The points represent experimental data and the lines show the fit of the data to a first order polynomial.

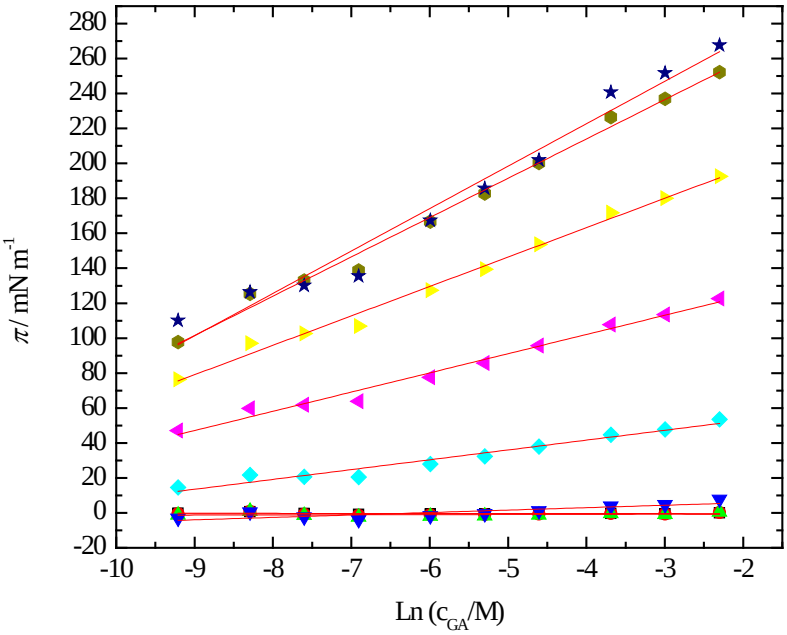

Fig. 7 Surface pressure π at a constant total charge plotted against the logarithm of the glycolic acid concentration. Points are the experimental data, lines show the best linear fit to the data. From the lowest to the highest curve, the charge density corresponds to -50, -25, 0, 25, 50, 75, 100, 125 and 150 μC cm^{-2}.

From the polynomial fitting is possible to calculate the Gibbs excess. It was previously demonstrated [12] that similar results are obtained when the analysis is performed for both charge and potential as the independent electrical variable. In this work, the charge was used as the independent variable because a better fit and smaller dispersion of data were observed.

The Gibbs excess of glycolate is plotted against the electrode potential in Fig. 8. As can be seen, the surface excesses increase progressively with potential. The curves display a well-defined plateau at Γ=6.0 x 10^{14} ions/cm^2. This number is equivalent to 0.4 monolayer (ML) coverage of the Pt(111) electrode surface by adsorbed anions. One ML corresponds to the surface concentration of Pt atoms at an ideal Pt(111) electrode surface equal to 1.5 x 10^{15} ions/cm^2. In Fig. 8 the only discordant value is that corresponding to the 10^{-4} M GA concentration.

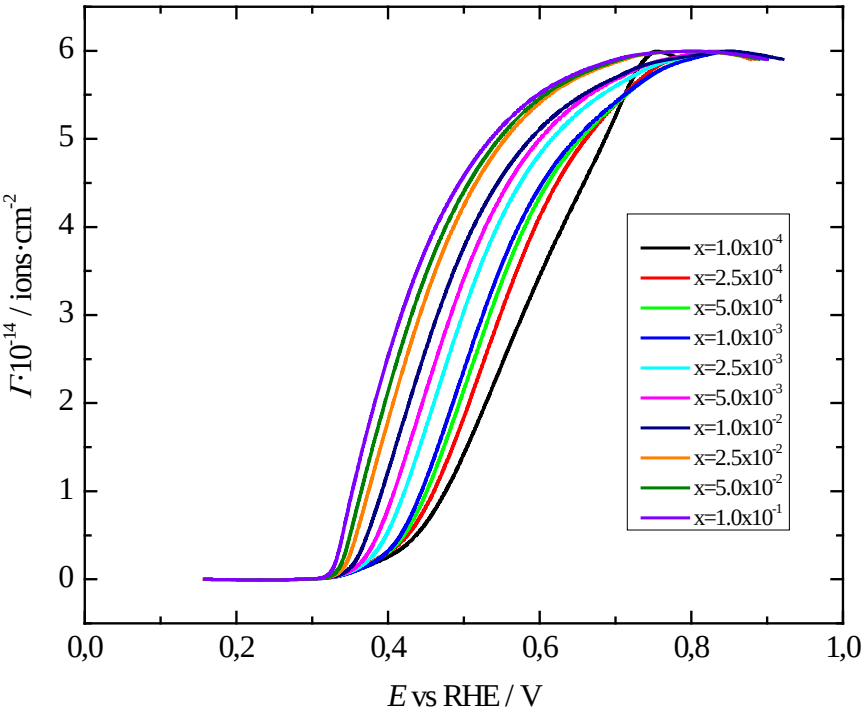

Fig. 8 Plot of the Gibbs excess of glycolic acid adsorbed at the Pt(111) electrode from *x* M GA + 0.1 M $HClO_4$, where *x* values are the same as in Fig. 4.

Another important parameter that can be calculated from this analysis is the charge number. Cross differenciation of the electrocapillary equation gives two charge numbers related to the number of electrons flowing to the electrode per one adsorbed anion [21]:

$$1/z_{\Gamma} = 1/z_{\Gamma,\Delta} \approx 1/z_{\Delta,\Gamma} \qquad (4)$$

and

$$1 \quad \Gamma = 1 \quad q \qquad (5)$$

where l is the charge number at a constant electrode potential and is usually known as the electrosorption valency, and n' is the charge number at a constant chemical potential. In Eqs. (4) and (5), q is the total charge, Γ is the Gibbs excess of adsorbed anion and μ is the chemical potential of the anion in the bulk solution. Fig. 9 shows the charge number at constant chemical potential defined by Eq. (5). Values in the region where adsorption process takes place are very close to -1, clearly indicating that one electron is transferred upon adsorption of one anion. At very low and high charge, (or potential for l) deviates from these value from the interference of other processes, especially hydrogen adsorption in the lower potential region.

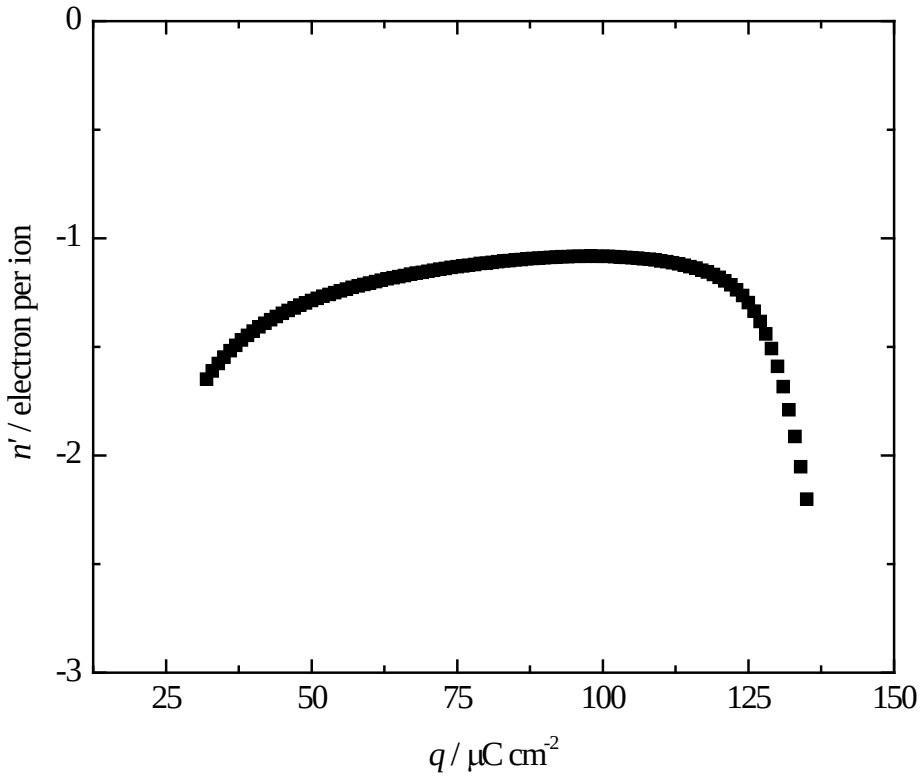

Fig. 9 Charge numbers at constant chemical potential, determined from the slope of q vs. Γ_{GA}, plotted against the total charge density.

Spectroelectrochemical results

As has been previously stated, some kinetic processes can be observed in the oxidation of GA. FTIR experiments were carried out with the aim of gaining insight into the nature of the species produced/involved in this reaction. In the following spectra, positive bands correspond to the products formed at the sampling potential, while negative bands are due to the consumption of species present at the reference potential. Fig. 10 shows the spectra taken for the Pt(111) electrode in a 0.1 M GA + 0.1 M $HClO_4$ solution. Reference spectra was taken at 0.2 V, prior to the anion adsorption. Although the band at 1620 cm^{-1}, related to the bending mode of the water, can be seen in some spectra, the important features related to the presences of GA are the following. (i) The band at 2343 cm^{-1} is due to the asymmetrical stretching mode of CO_2 in solution; the band is already visible at low potentials, pointing out that the complete oxidation of the molecule of GA to CO_2 takes place. These results assert that GA is more oxidable than acetic acid, where no C-C bond cleavage is observed, and this should be associated with the presence of the OH electron abstractor group in the GA molecule. (ii) The bands at 1724 cm^{-1} and 1271 cm^{-1} corresponds, respectively, to the C=O stretching of a carbonyl group and the C-O stretching + OH deformation of a carboxylic acid group. These bands can be linked to the presence of glycolic acid but also to the formation of oxalic acid. The presence of this latter molecule could be corroborated by the band at 1635 cm^{-1}, corresponding to the ν_{as}(OCO) mode of bioxalate observed at 0.7 V. In the spectra obtained, the water hides any band present in this region. Nevertheless, in a previous work [7] it was demonstrated the formation of oxalic acid from the oxidation of the alcohol group of the glycolic acid molecule. (iii) The band at 1398 cm^{-1} is assigned to adsorbed glycolate [22,23], and is present in all the spectra taken between 0.3 V and 0.95 V, clearly related to the adsorption of the anion, discussed in previous paragraphs.

It should be highlighted that the bands associated to adsorbed CO are completely absent in all the spectra, pointing out that the C-C breaking of the glycolic acid leads to the direct formation of CO_2 without poisoning the surface of the electrode. When the cleavage takes

place, the fragment containing the carboxylic group will evolve immediately to yield CO_2. The presence of CO_2 only above 0.5 V suggest that the cleavage is only occurring above this potential, unlike ethanol or ethylene glycol oxidation, where the cleavage occurs at low potentials [7,24,25]. The fragment with the alcoholic group will require and additional O group to yield CO_2 and probably evolves through the formation of CO, as observed for ethanol [24]. The absence of adsorbed CO probably is associated to the rapid oxidation of CO, since the cleavage occurs at potentials where CO oxidation can take place.

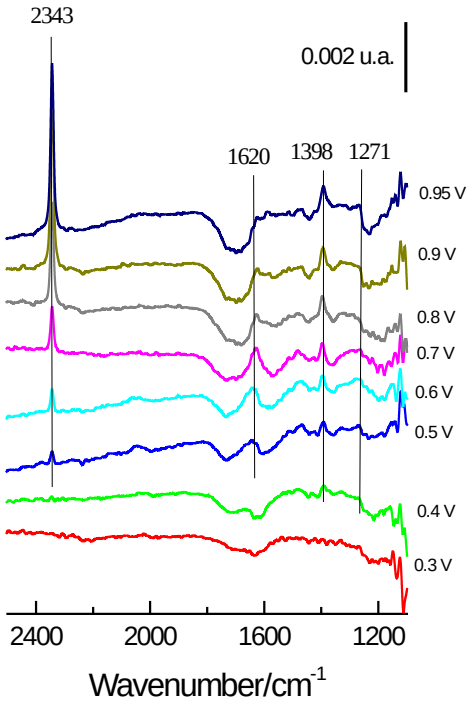

Fig. 10 FTIR spectra obtained for the Pt(111) electrode at different potentials, as labeled, in 0.1 M GA + 0.1 M $HClO_4$. The reference spectra was taken at 0.2 V.

Conclusions

We have described the influence of the sweep rate and the bulk concentration on the glycolic acid oxidation reaction. The presence of an extra OH group in the molecule of glycolic

acid makes it more reactive on the Pt(111) surface in comparison with acetic acid. In this way, while only adsorption processes take place with acetic acid, in the case of glycolic acid is possible to distinguish between the thermodynamically controlled processes (hydrogen and anion adsorptions) and the kinetically controlled processes (glycolic acid oxidation), as represented in Scheme 1.

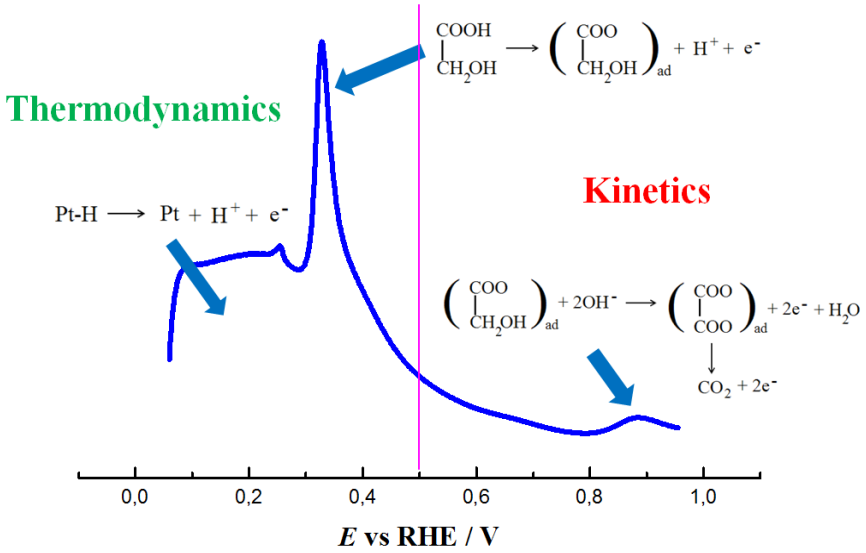

Scheme 1. Voltammetric profile of Pt(111) electrode in .1 M GA + 0.1 M $HClO_4$ solution, 50 mV s^{-1}. Thermodynamic processes take place above 0.5 V while kinetics occurs below this potential. Arrows point out the reaction that take place in each potential region.

Using conditions where kinetic processes are absent, the surface Gibbs excess and the charge numbers for the adsorption of glycolate were determined. The results show that the maximum Gibbs excess of glycolate attains a reaches a value of ~ 6.0 $\times 10^{14}$ ions/cm^2, which corresponds to the packing density of ~ 0.4 ML and one electron is transferred per adsorbed anion. On the other hand, the oxidation process has been characterized using FTIR. These experiments points out that on the surface of the Pt(111) electrode both adsorption and oxidation of glycolic acid take place, producing CO_2 and possibly oxalic acid.

Acknowledgements

The work was carried out under the financial support by the MINECO (Spain) (project CTQ2013-44083-P) and Generalitat Valenciana (project PROMETEOII/2014/013).

References

1. Clavilier J, Faure R, Guinet G, Durand R (1980) J Electroanal Chem 107:205-209

2. Clavilier J (1980) J Electroanal Chem 107:211-216

3. Berna A, Climent V, Feliu JM (2007) Electrochem Commun 9:2789-2794

4. Rizo R, Herrero E, Feliu JM (2013) Phys Chem Chem Phys 15:15416-15425

5. Jaaf-Golze KA, Kolb DM, Scherson D (1986) J Electroanal Chem 200:353-362

6. Colmati F, Tremiliosi-Filho G, Gonzalez ER, Berna A, Herrero E, Feliu JM (2008) Faraday Discuss 140:379-397

7. Arán-Ais R.M, Herrero E, Feliu JM (2014) (2014) Electrochem Commun 45:40-43

8. Arán-Ais RM, Abe Santos N, Villullas HM, Feliu JM (2013) ECS Trans 53:11-22

9. Herrero E, Mostany J, Feliu JM, Lipkowski J (2002) J Electroanal Chem 534:79-89

10. Mostany J, Herrero E, Feliu JM, Lipkowski J (2002) J Phys Chem B 106:12787-12796

11. Mostany J, Herrero E, Feliu JM, Lipkowski J (2003) J Electroanal Chem 558:19-24

12. Garcia-Araez N, Climent V, Herrero E, Feliu J, Lipkowski J (2005) J Electroanal Chem 576:33-41

13. Clavilier J, Armand D (1986) J Electroanal Chem 199:187-200

14. Rodes A, Pastor E, Iwasita T (1994) J Electroanal Chem 376:109-118

15. Garcia-Araez N, Lukkien JJ, Koper MTM, Feliu JM (2006) J Electroanal Chem 588:1-14

16. Orts JM, Rodes A, Feliu JM (1997) J Electroanal Chem 434:121-127

17. Angelucci CA, Souza-Garcia J, Herrero E, Feliu JM (2010) J Electroanal Chem 646:100-106

18. Climent V, Garcia-Araez N, Herrero E, Feliu JM (2006) Russ J Electrochem

19. Savich W, Sun SG, Lipkowski J, Wieckowski A (1995) J Electroanal Chem 388:233-237

20. Parsons R (1961) Proceedings of the Royal Society of London Series A, Mathematical and Physical Sciences 261:79-90

21. Trasatti S, Parsons R (1986) J Electroanal Chem 205:359-376

22. De Lima RB, Paganin V, Iwasita T, Vielstich W (2003) Electrochim Acta 49:85-91

23. Christensen PA, Hamnett A (1989) J Electroanal Chem 260:347

24. Souza-Garcia J, Herrero E, Feliu JM (2010) ChemPhysChem 11:1391-1394

25. Del Colle V, Souza-Garcia J, Tremiliosi G, Herrero E, Feliu JM (2011) Phys Chem Chem Phys 13:12163-12172